International Journal of Computing and Digital Systems
ISSN (2210-142X)
Int. J. Com. Dig. Sys. 11, No.1 (Jan-2022)

https://dx.doi.org/10.12785/ijcds/110135

Network Constraints Economic Dispatch of Renewable Energy Sources with Impact of Energy Storage

Bharat Singh[1] **and Ashwani Kumar Sharma**[2]

[1]*Department of Electrical Engineering, National Institute of Technology, Kurukshetra, India*
[2]*Department of Electrical Engineering, National Institute of Technology, Kurukshetra, India*

Received 29 Aug. 2020, Revised 24 Nov. 2021, Accepted 4 Jan. 2022, Published 20 Jan. 2022

Abstract: The distributed energy sources and the energy-storage system are considered a critical solutions for integrating renewable energy sources in Microgrids. The optimal size of battery storage is essential to overcome the intermittency of Renewable energy sources for energy-saving and cost-benefit. The present paper addresses the determination of optimal sizing of the battery energy storage system (BESS) in a dis-patchable and non-dis-patchable energy sources based micro-grid. The main contribution of the paper is:
(i) to obtain an optimal size of battery energy storage in a combined heat and power (CHP), Micro-Turbine (MT), Fuel Cell (FC), Wind Turbine (WT) and Solar Photovoltaic (PV) based hybrid system (ii) to determine the impact of renewable and Distributed Generation (DGs) on the sizing of BESS (iii) Optimal scheduling of dispatchable units (iv) The dispatchable schedule of CHP, MT and FC with ramp rate control. The hourly spinning reserve, minimum up, and down-time constraints have been taken into account. In addition, a linear piecewise cost function is considered for the cost-benefit analysis. The minimum daily energy loss profile, voltage, and power loss have been obtained. The state of charge (SOC) of battery profile, the cost of battery energy per day, unit commitment (UC) cost, startup, and shunt down cost have also been determined. The proposed technique has been tested on the IEEE-33 bus test system considering realistic ZIP load. The general algebraic modelling system (GAMS) was used to solve an optimization problem. The increment in total benefit obtained is 11.44% with using battery energy storage. The annual cost of energy loss saving of $62448.51 (61.99%) has been obtained, and the increment in minimum voltage obtained is 2.831% with the proposed technique for the 33 bus test system.
Keywords: Battery Storage System, Daily Energy Loss, Renewable Energy Sources, Total Benefit, Unit Commitment, Piecewise linear function,

1. Introduction

In recent years, considerable attention has been focused on the intermittency of renewable-based MG generation on a large scale. The MG architecture consists of the group of the radial feeder with the distribution network, which has a single point of connection called the point of common coupling (PCC). The MG also has renewable energy sources consisting of a Micro-Turbine (MT) system, Wind-Turbine (WT), Solar Photovoltaic (PV) system, a Fuel cell (FC), combined heat and power (CHP) system, and the energy storage system. The fuel input is needed only for the FC, MT, and CHP, whereas the energy input for the PV and WT comes from the sun and wind. The upstream and downstream (.i.e. MG) can be served the load directly with the energy sources, likewise FC/WT/MT/CHP and PV in grid-connected mode. The energy management has been operated between the upstream Grid and MG by a smart energy management controller (central controller). Furthermore, the central controller must control the power output and build the coordination between the central and local controller for optimal power generation.

The intermittent nature of renewable energy sources (RES) and MG has constituted a controlling task for MG challenges. The uncertain nature of RESs with load demand, power deficiency and voltage stability problems have to be solved. In this context, the energy storage device has been identified for the solution aspect. Therefore, the profitability system cost-based analysis was studied for the location and size of ESS [1]. Furthermore, the FC/WT/MT/CHP and PV energy sources are required to solve the influence of BES. In the present hybrid power network with renewable energy sources and storage devices, the appropriate utilization of dispatchable and non-dispatchable generation must be considered for deciding the optimal sizing of storage devices.

The main motivation of this work is to determine the sizing of energy storage. In recent literature did not consider the following points;

1) The precise size of BES has not been considered with the combination of CHP, PV, WT, MT and FC along with ZIP load.
2) Many researchers have considered the linear cost

E-mail address: bharat7091988@gmail.com, ashwaks@gmail.com

function, but most did not consider the piecewise linear cost function for the generation cost.
3) The unit commitment problem has to be considered for the optimal scheduling of the dis-patchable units.
4) The spinning reserve with the hourly load demand has to be considered along with renewable energy sources.

In this paper, all points, as mentioned above, have been carried out for analysis. The multi-objective scenario has been taken along with the proposed algorithm for the solution.

The energy storage devices and their optimal sizes have become the essential requirement for MG operators to meet the power mismatch as well as the support of power intermittency in renewable energy integrated systems. Chen, S. X et al. [2] were analyzed the BES by unit commitment problem for MG reserve power. The time series based analysis was used for the PV and WT. However, the ramp rate constraints with minimum time were not considered. The BES sizing problem has also been considered using the Bat algorithms to solve the unit commitment (UC) problem with FC MT and CHP [3].

However, In [4], the stochastic problem had been represented for the intermittent nature of RES for loss minimization. The BES has been considered along with PV, WT, MT, FC and the diesel generators to stabilize energy dispatch strategy in [5], although the sizing of BES and CHP was not considered. In literature [6], the iterative method along with the cost-benefit, UC for the dis-patchable units, and piecewise linear cost function were not considered for the optimal sizing of BES with the influence of the renewable-based generation (CHP/FC/MT). Although, the outer and inner layer optimization were used for enhancement of voltage-regulation in distribution with network considering the BES and DG. The energy storage component also plays an essential role in the renewable-based sources for the virtual energy hub pant consisting of PV/WT/CHP [7].

The economic dispatch of microgrid had been solved for battery energy storage (BES), using the mixed-integer non-linear (MINLP) approach in [8]. The Combined heat and power units were used for serving the residential load by evaluating the demand response programming in [9]. The optimal dispatch of CHP based generation with energy storage was represented for the determination of energy reserve in [10]. The impact of the renewable energy sources market was proposed in [11] for stochastic modelling of CHP-based microgrid. The WT, PV, CHP and BES have been considered for cost-based analysis to ensure maximum profit and minimum emission [12]. In the literature mentioned from [8] to [11], the CHP based DG has been taken into account; however, the BES has not been considered.

The CHP-based distribution generation and BES coordination were proposed in [13] to [14]. The particular type of battery has been analyzed and tested with CHP also. The energy cost minimization problem was addressed for the full utilization of CHP and battery storage system [14]. The wind turbine power fluctuations were considered for determining the sizing of the BES using the probabilistic approach [15]. The Monte Carlo simulation (MCS) was addressed for dispatching MG with a cost-based rule [16]. For modelling of the solar radiation, the Monte Carlo Simulation was utilized in [17]. Mostafa H. Aleem [18], presented the stochastic optimization approach for uncertainty in market price and analyzed the impact of different types of battery storage systems. The cost reduction has been achieved up to 40% with considering BES for the uncertainty model of renewable-based generation [19]. In literature [20], the Techno-economical based analysis has been carried out for the dispatch analysis considering the RES and BES.

The energy management approach was proposed in [21] for the coordination of CHP and PV systems. The GAME theory approach was used for obtaining the optimal strategy. The authors proposed a rolling dispatch strategy for the CHP installation in an uncertain scenario [22]. In this contrast, the online energy storage scheduling along with the CHP-based system was represented in [23], solving the non-convex optimization problem, although the impact of BES has not been considered.

Some recent papers addressed the issue of power loss savings for MG [24]. The volt/Var analysis was used for the Solar PV installation using the MINLP based approach to determine the economic dispatch problem in [25]. The energy loss had calculated through load means and load variance for low voltage networks [26]. The simultaneous optimization technique was presented to install DGs for minimizing power loss and voltage deviation [27].

In paper [28], the demand-side biding of the controllable load problem has been solved with the priority-based UC problem. In paper [29], diesel generators and a combination of ESS have been concluded for the reduction in the cost of UC. The reserve management approach for a microgrid and sensitivity analysis for spinning reserves of FC and MT have been proposed in [30]. Using piecewise linear approximation constraints, the low voltage grid-connected battery storage system has been considered for power loss minimization [31]. Paper [14] to [18], presents various optimization techniques to size BES and install renewable-based DGs [32]. The literature [33] and [34] discussed the different algorithms and techniques to minimize the power loss with BES and the RES.

The central key points of the above literature survey have been summarized based on the literature review as follows:

1) A combination of PV/WT/FC/MT&CHP for the energy-saving and total benefit did not consider the BES sizing.
2) Most of the researchers are trying to implement

the UC problem and the BES, but very few have considered the piecewise linear cost function and UC cost.
3) The two-layer model has to consider the cost-based as well as energy-saving based issue.
4) The previous work has not proposed a decision-making process for the microgrid system operator to optimize BES.

As per the mentioned literature, in this paper, the research gap has been fulfilled as follows:

1) Simultaneous optimization of cost of generation, the total benefit, energy saving have been performed.
2) The solar PV has been modelled using the Monte Carlo Simulation.
3) The market profit cost-based analysis has been implemented with a linear piecewise cost function of dispatchable units.
4) The two-layer optimization problem has been solved for the sizing of BES in the UC scenario.
5) The UC problem has been solved by considering the ramp rate constraints, minimum up/downtime constraints, hourly spinning reserve, and linear piecewise cost function.
6) The daily energy loss, voltage profile, power loss profile, along with the State of Charge (SOC) of BES, have been determined for the distribution network.

In this paperwork, the previous work of paper [35] has been extended along with the BES system in a hybrid system comprising of the Fuel cell (FC), CHP, Micro-Turbine (MT), Wind Turbine and solar-based RES. The proposed technique has been tested on the IEEE-33 bus test system considering a realistic ZIP load model. The optimization problem has been solved using the general algebraic modelling system (GAMS) [36].

The paper is organized in the following sections as; Section 2 represents the proposed work problem formulation and mathematical modelling. The algorithm developed for solving the multi-objective optimization problem is elaborated in Section 3. The data used in this paper is given in Section 4. In Section 5, the results and discussions are discussed. Finally, the conclusion of the work is given in Section 6.

2. PROBLEM FORMULATION

In this proposed work, the objective function consists of the outer and inner layer optimization problems. The outer layer optimization has considered the determination of optimal sizing of battery energy storage. The BES size has been obtained considering Micro-Turbine (MT), Fuel Cell (FC), Combined Heat and Power (CHP), and PV and WT.

Objective (i): to maximize the market benefit, including the total benefit and cost of battery per day.

Objective (ii): the daily energy loss has been minimized for the distribution network.

Objective (iii): the generation cost has been minimized.

The multi-objective problem has consisted of the outer layer model being solved to obtain the location and BES size using the iterative method. In the outer layer, the decision variables are considered as (i) the battery cost per day, (ii) market benefit and Total benefit (TB) (iii) the unit commitment cost of the dispatch-able units.

The outer layer optimization has been solved for cost-benefit based simulation along with a piecewise linear cost model. After obtaining the optimal size of BES from the outer layer, the inner layer model has again been solved for obtaining the variables for BES (as explained in section 2.1.2). In the inner layer model, the decision variables are the size of battery energy storage (BES), number of BES, state of charge (SOC) of BES, BES charging/discharging power, number of cost segments and power outputs of RES. The outer and inner layer optimization problem has been solved using mixed-integer non-linear programming (MINLP) with MATLAB and GAMS interfacing.

A. Mathematical Model

In this section, the mathematical formulation has consisted of the outer layer and inner layer optimization problems formulation as follows;

1) Modelling of Outer Layer

In the outer layer, the multi-objective problem is solved for determining the optimal size and location of BES as follows:

$$max\{f_1\} = Market_{Benefit} - Batt_{CPD} \tag{1}$$

$$min\{f_2\} = \sum_{k}^{T}\sum_{i}^{nb} G_{ij}^{k}\left\{(V_i^k)^2 + (V_i^k)^2 - 2V_i^k V_j^k \bullet cos\left(\delta_i^k - \delta_j^k\right)\right\} \tag{2}$$

$$Market_{Benefit} = \sum_{k}^{T}\left\{Price_{Market} \bullet \sum_{i}^{nb}\left(P_{gen_i}^{k}\right) - UCC_{disp}\right\} \tag{3}$$

$$Batt_{CPD} = \left\{\left(\frac{rt.(1+rt)^{yr}}{(1+rt)^{yr}-1}\right)\bullet Batt_{fc} + Batt_{MC}\right\} \bullet \frac{(Batt_{Size} * Nbatt)}{365} \tag{4}$$

$$UCC_{disp} = \sum_{k}^{T}\sum_{i}^{nb}\left\{rRn_{i,k} + Cost_{i,k}^{gen} + \left(U_{i,k}^{wind} voll^{wind}\right) \bullet P_{i,k}^{wind} + \left(U_{i,k}^{PV} voll^{PV}\right) \bullet P_{i,k}^{PV}\right. \tag{5}$$

The objective function consists of market benefit and battery cost per day. The Equations 1 and 2 are the objective functions. These equations are simultaneously optimized using the Pareto method in GAMS. The market benefit is

determined using The Equations 1, and 3. The battery cost per day is represented in Equation 4. Equation 5 gives the unit commitment cost for the dis-patchable units. $Cost_{i,k}^{gen}$ is operating cost of generation units (inner layer). where $Nbatt$ is number of battery energy storage.

2) Modelling of Inner Layer

In the inner layer model, the cost of generating units are minimized by considering the daily energy saving. The objective function is given for the inner layer model in Equation 6.

$$min\left\{Cost_{i,k}^{gen}\right\}=STC_{i,k}^{gen}+SDC_{i,k}^{gen}+$$

$$\mathrm{U}_{i,k}^{gen}\left\{a_i(P_{gen_i}^{\ k})^2+b_iP_{gen_i}^{\ k}+c_i\right\}+\sum_{sg}^{nsg}\left\{s_i^{sg}\Delta P_{i,k}^{sg}\right\} \quad (6)$$

In GrindEQ$_{6 theterm}\sum_{sg}^{nsg}\left\{s_i^{sg}\Delta P_{i,k}^{sg}\right\}$ represents the piece-wise linear cost function parameter. The $STC_{i,k}^{gen}$ and $SDC_{i,k}^{gen}$ are represented as the startup and shutdown cost for generating units, respectively. In this context, the following equality and inequality constraints equations are considered in the inner layer as follows:

a) Power balance equations

$$P_i^k=\left(Pg_i^k+Pgrid_i^k-Pd_{ZIP,i}^k\right)=$$

$$\mathrm{V}_i^k\sum_{j=1}^{n}V_j^k\left(G_{ij}^k cos\left(\delta_i^k-\delta_j^k\right)+B_{ij}^k sin\left(\delta_i^k-\delta_j^k\right)\right) \quad (7)$$

$$Q_i^k=\left(Qg_i^k+Qgrid_i^k-Qd_{ZIP,i}^k\right)=$$

$$\mathrm{V}_i^k\sum_{j=1}^{n}V_j^k\left(G_{ij}^k sin\left(\delta_i^k-\delta_j^k\right)-B_{ij}^k cos\left(\delta_i^k-\delta_j^k\right)\right) \quad (8)$$

$$\forall\ i\in S_B\ \&\ k\in S_T$$

b) Power generation equations

$$Pg_i^k=P_{gen,i}^k+N_{wind}(i)\bullet P_{wind_i}^{\ k}$$

$$+\mathrm{N}_{PV}(i)\bullet P_{PV_i}^k+N_{batt}(i)\bullet\left(P_{ch_i}^{\ k}-P_{dis_i}^{\ k}\right) \quad (9)$$

$$Qg_i^k=Q_{gen_i}^{\ k}+N_{wind}(i)\bullet Q_{wind_i}^{\ k} \quad (10)$$

c) Ramp rate constraints for the generation

The ramp rate constraints for the generating units are:

$$P_{gen_i}^{\ k}\le\ P_{gen_{i,k}}^{max}\left[U_{i,k}^{gen}-X_{i,k+1}^{gen}\right]+\ SD_{i,k}^{gen}\bullet X_{i,k+1}^{gen} \quad (11)$$

$$P_{gen_i}^{\ k}\le P_{gen_i}^{\ k-1}+RU_{i,k}^{gen}\bullet U_{i,k-1}^{gen}+\ SU_{i,k}^{gen}\bullet Y_{i,k+1}^{gen} \quad (12)$$

$$P_{gen_i}^{\ k}\ge P_{gen_{i,k}}^{min}U_{i,k}^{gen} \quad (13)$$

$$P_{gen_i}^{\ k}\ge P_{gen_i}^{\ k-1}-RD_{i,k}^{gen}\bullet U_{i,k}^{gen}-\ SD_{i,k}^{gen}\bullet X_{i,k}^{gen} \quad (14)$$

Where, $SU_{i,k}^{gen}$ and $SD_{i,k}^{gen}$ are the startup and shut–down cost constants for the generating units for ith bus at kth time. Equation 11 represents the upper operating limits for the generating units for the ith bus at the kth time. If the ith generating unit shutdown in the next hour(k + 1): $P_{gen_i}^{\ k}\le SD_{i,k}^{gen}\bullet X_{i,k+1}^{gen}$. Since,$P_{gen_i}^{\ k+1}=0$, so that $P_{gen_i}^{\ k}$ is not more than $SD_{i,k}^{gen}$ [37]. In Equation 12, the ith generating unit cannot be increased more than $RU_{i,k}^{gen}$ as represents$P_{gen_i}^{\ k}\le(P_{gen_i}^{\ k-1}+RU_{i,k}^{gen}\bullet U_{i,k-1}^{gen})$, if the unit has been on the previous hours ($U_{i,k-1}^{gen}=1$). Therefore, the generating unit remains on if it has been on for the previous hour. If the generating unit has been off in the prior hour ($U_{i,k-1}^{gen}=0$) and it is being on at time (k) i.e.($Y_{i,k}^{gen}=1$), than $P_{gen_i}^{\ k}$ is not more than $SU_{i,k}^{gen}$.

Equations 13 and 14 represents the minimum time constraints of generating unit. In Equation 13, the generated power is higher than the minimum power limit if the generating units are on. In Equation 14, to remain the units on at time k; the minimum generated power is $(P_{en_i}^{\ k-1}-RD_{i,k}^{gen}\bullet U_{i,k}^{gen})$. The generated power is being lower than $(SD_{i,k}^{gen}\bullet X_{i,k}^{gen})$; if the unit is on at time $k-1$ and turned off at time k.

d) Startup/Shutdown cost constraints

$$Y_{i,k}^{gen}-X_{i,k}^{gen}=U_{i,k}^{gen}-U_{i,k-1}^{gen};Y_{i,k}^{gen}+X_{i,k}^{gen}\le 1 \quad (15)$$

$$STC_{i,k}^{gen}=Cost_{i,k}^{ST}Y_{i,k}^{gen} \quad (16)$$

$$SDC_{i,k}^{gen}=Cost_{i,k}^{SD}X_{i,k}^{gen} \quad (17)$$

e) Startup/Shutdown Time constraints

Minimum up time (UT_i) constraints are modelled as;

$$\sum_{k}^{T-UT_i+1}\left(1-U_{i,k}^{gen}\right)=0;$$

$$\sum_{k=sg}^{sg-UT_i+1}\left(U_{i,k}^{gen}\right)\ \ge\ UT_i\bullet Y_{i,k}^{gen}\ ;$$

$$\sum_{k=sg}^{T}\left(1-Y_{i,k}^{gen}\right)\ \ge\ 0;\forall\ sg=T-UT_i+2\ldots..T \quad (18)$$

Minimum downtime (DT_i) constraints are modelled as;

$$\sum_{k}^{T-UT_i+1}\left(U_{i,k}^{gen}\right)=0;$$

$$\sum_{k=sg}^{sg-UT_i+1}\left(1-U_{i,k}^{gen}\right)\ \ge\ DT_i\bullet X_{i,k}^{gen}$$

$$\sum_{k=sg}^{T}\left(1-U_{i,k}^{gen}-X_{i,k}^{gen}\right)\ \ge\ 0;$$

$$\forall\ sg=T-DT_i+2\ldots..T \quad (19)$$

where, $U_{i,k}^{gen},X_{i,k}^{gen},Y_{i,k}^{gen},\in(1,0)$, are the binary variables.

f) Power Loss equation

$$\left|P_{ij}^{k}\right| = \left|\sum_{k}^{T}\sum_{i}^{nb} G_{ij}^{k}\left\{(V_i^k)^2 + (V_i^k)^2 - 2V_i^k V_j^k \bullet cos\left(\delta_i^k - \delta_j^k\right)\right\}\right| \leq \left|Pl_{max}^{k}\right| \quad (20)$$

Inequality constraints:

g) Capacity Limits of the generation system

$$P_{Gi}^{min} \leq Pg_i \leq P_{gi}^{max}, \quad i \in S_G \quad (21)$$

$$Q_{gi}^{min} \leq Qg_i \leq Q_{gi}^{max}, \quad i \in S_G \quad (22)$$

h) Voltage and angle limits

$$V_{i,k}^{min} \leq V_i^k \leq V_{i,k}^{max}, \quad i \in S_B$$
$$\delta_{min_i}^{\ k} \leq \delta_i^k \leq \delta_{max_i}^{\ k}, \quad (23)$$
$$\forall i = 1, 2 \ldots .nb$$

i) Power factor limits

$$pf_i^{lo} \leq pf_i \leq pf_i^{up}, \quad i \in S_B \quad (24)$$

j) Energy storage constraints

$$SOC_i^{min}(k) \leq SOC_i(k) \leq SOC_i^{max}(k) \quad (25)$$

$$SOC_i^{max}(1) = 0.90 * N_{bat}(i) Batt_{Size} \quad (26)$$

$$SOC_i^{max}(24) = 0.90 * N_{bat}(i) Batt_{Size} \quad (27)$$

$$0 \leq P_{ch_i}^{\ k} \leq 0.6 \bullet N_{bat}(i) Batt_{Size} \quad (28)$$

$$0 \leq P_{dis_i}^{\ k} \leq 0.6 \bullet N_{bat}(i) Batt_{Size} \quad (29)$$

$$P_{dis_i}^{\ k} \bullet P_{ch_i}^{\ k} = 0 \quad (30)$$

B. Mathematical Modelling of RES

In this section, the mathematical modelling of BES, Solar PV, WT, FC, MT, and CHP, has been formulated as follows;

1) PV Panel modelling

The solar PV-based RES of 48 V DC has been carried out for analysis. The PV modelling is obtained using the MCS. In MCS, the 1000 samples are generated for tracking of maximum power point [17]. The solar PV model is:

$$P_{solar}\left(I_\beta\right) = N_{PV} \bullet P_{rated}^{PV} \frac{G}{G0} \bullet \{1 - T_c\,(T_A - 25)\} \bullet \eta_{inv}\eta_{rl} \quad (31)$$

where, η_{inv} and $,\eta_{rl}$ are the efficiency of inverter and renewable energy sources, i.e. PV. In Figure 1, the power output of solar PV for 24 hours is depicted.

2) Wind Power modelling

The quadratic wind model is represented as in Equation 32. The variation of wind velocity with WT power generated is depicted in Figure 2.

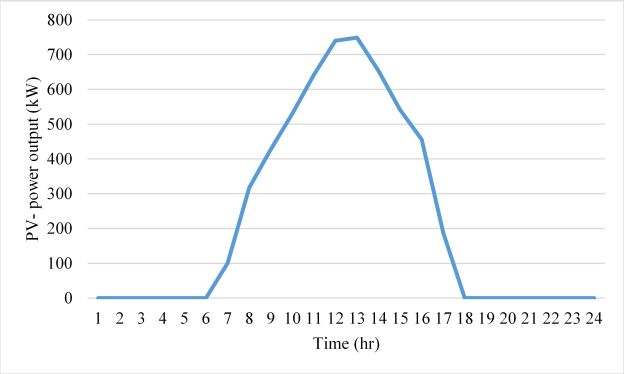

Figure 1. Hourly power output curve of solar PV

$$P_{wind} = \begin{cases} P_{rated} \bullet \left((v - v_{in})^2/(v_r - v_{in})^2\right) \; ; \; v_{in} \leq v \leq v_r \\ P_{rated}; \; v_r \leq v \leq v_{out} \\ 0; \quad v > v_{out} \; and \; v < v_{cut} \end{cases} \quad (32)$$

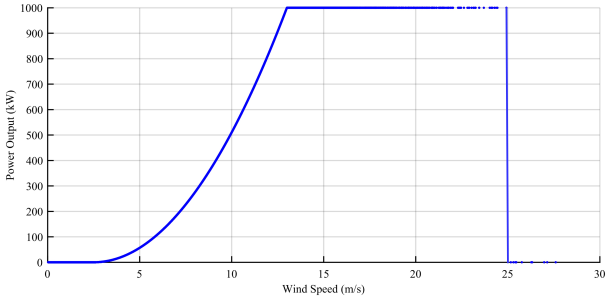

Figure 2. The power generation of wind Turbine with wind speed

3) Energy storage modelling

In this paper, the BES is taken out as the energy storage system. The minimum and maximum battery discharge power are represented in Equation 33 and 34. The state of charge (SOC) is calculated by using Equation 35.

$$SOC_{min} = N_{bat} Batt_{size}\,(1 - DOD_{max\_bat}) \quad (33)$$

$$SOC_{max} = N_{bat} Batt_{size} \quad (34)$$

$$SOC\,(i, k + \Delta k) = \mathrm{SOC}(i,k)\,.\,(1 - \delta) + \left(P_{ch_i}^{\ k}.\eta_{ch} - P_{dis_i}^{\ k}.1/\eta_{dis}\right).\Delta k \quad (35)$$

The charging and discharging schedule of battery energy storage has been decided by the amount of energy available for the time duration of Δt. The discharging schedule of battery storage depends on peak energy saving. The battery

has discharge only if the renewable energy and dispatchable generators, likewise FC and MT (in this paper) is not able to supply the load. The battery schedule for charging and discharging is modelled with SOC as represented in Equations 36 and 37, respectively.

$$E_{dis_{i,k}}^{min} = \int_{k}^{T} \left(Pd_{Load,i}^{k} - \max\left(Pgrid_{i}^{k}\right) - \max(P_{gen\,i}^{k})\Delta t; if\ Pd_{Load,i}^{k} \geq \max\left(Pgrid_{i}^{k}\right)\right) \quad (36)$$

The charging energy of BES is based on the peak energy-saving mode of operation. If the load demand is lower than the maximum power drawn from the grid, the battery has been charged.

$$E_{ch_{i,k}}^{min} = \int_{k}^{T} \left(\max\left(Pgrid_{i}^{k}\right) + \max\left(P_{gen_{i}}^{k}\right) - \mathrm{Pd}_{Load,i}^{k}\Delta t;\ if\ Pd_{Load,i}^{k} \leq \max\left(Pgrid_{i}^{k}\right)\right) \quad (37)$$

4) Fuel Cell Model

The Fuel cell (FC) is the best example of clean energy as the requirement of conventional fuel is not required. Therefore, the FC is carried out for the analysis the cost function is depicted in Equation 38 as:

$$Cost_{FC} = \left(\frac{P_{gen_{i}}^{FC}}{\eta_{FC}}\right) Csu_{fuel\_FC} \quad (38)$$

where, Csu_{fuel_FC} is a price to supply of fuel ($/kWh).

5) Micro-Turbine Model

The conventional heat engine, with lower installation cost, small size, higher reliability, lower cost of maintenance and higher efficiency based Micro-turbine (MT), is carried out. The cost function of MT consists of fuel cost, efficiency and power generation as given in Equation 39.

$$Cost_{MT} = \left(\frac{P_{gen_{i}}^{MT}}{\eta_{MT}}\right) Csu_{fuel\_MT} \quad (39)$$

where, Csu_{fuel_MT} is a price to supply of fuel ($/kWh).

6) Piecewise linear cost model for MT and FC

The non-linear cost function has been solved as a linear cost function using the pice-wise linear model approach [37]. In this approach, the non-linear function is converted into a small number of segments (nsg) called the pice-wise cost segments, later these segments are solved individually, to make it a linear function.

$$0 \leq P_{i,k}^{sg} \leq \Delta P_{i,k}^{sg} \bullet U_{i,k}^{gen};\ \forall\ sg \in nsg \quad (40)$$

$$\Delta P_{i,k}^{sg} = \frac{\left(P_{gen_{i,k}}^{max} - P_{gen_{i,k}}^{min}\right)}{nsg} \quad (41)$$

$$P_{i,k,ini}^{sg} = (sg-1)\,\Delta P_{i,k}^{sg} + P_{gen_{i,k}}^{min} \quad (42)$$

$$P_{i,k,final}^{sg} = \Delta P_{i,k}^{sg} + P_{i,k,ini}^{sg}(43) P_{gen_{i,k}}^{min} \bullet U_{i,k}^{gen} + \sum_{sg}^{nsg}\left\{\Delta P_{i,k}^{sg}\right\} \quad (43)$$

$$Cost_{gen_{i,k,ini}}^{sg} = \left\{a_i(P_{i,k,ini}^{sg})^2 + b_i\ P_{i,k,ini}^{sg} + c_i\right\} \quad (44)$$

$$Cost_{gen_{i,k,final}}^{sg} = \left\{a_i(P_{i,k,final}^{sg})^2 + b_i\ P_{i,k,final}^{sg} + c_i\right\} \quad (45)$$

$$s_{i}^{sg} = \frac{\left(Cost_{gen_{i,k,final}}^{sg} - Cost_{gen_{i,k,ini}}^{sg}\right)}{\Delta P_{i,k}^{sg}} \quad (46)$$

$$Cost_{fuel}^{gen} = U_{i,k}^{gen}\left\{a_i(P_{gen_{i}}^{k})^2 + b_i P_{gen_{i}}^{k} + c_i\right\} + \sum_{sg}^{nsg}\left\{s_{i}^{sg}\Delta P_{i,k}^{sg}\right\} \quad (47)$$

$$\forall\ gen \in (FC,\ MT)$$

7) CHP Model

The combined heat and power (CHP) unit is modelled as follows; Figure 3, the operating region for chp1 and chp2

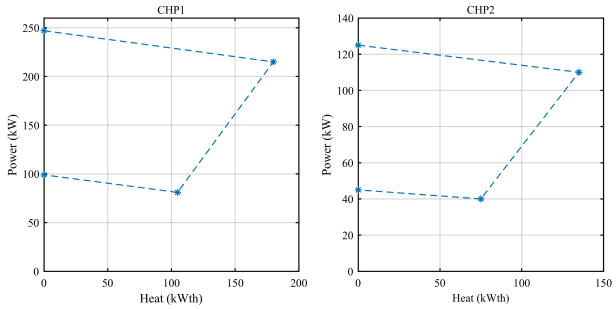

Figure 3. Operating region for CHP units

are shown. The linear relationship for the active region for CHP units are represented as follows;

$$P_{N,bus,k}^{CHP} - P_{N,bus,A}^{CHP} - \frac{\left(P_{N,bus,A}^{CHP} - P_{N,bus,B}^{CHP}\right)}{\left(H_{N,bus,A}^{CHP} - H_{N,bus,B}^{CHP}\right)}\left(H_{N,bus,k}^{CHP} - H_{N,bus,A}^{CHP}\right) \leq 0 \quad (48)$$

$$P_{N,bus,k}^{CHP} - P_{N,bus,B}^{CHP} - \frac{\left(P_{N,bus,B}^{CHP} - P_{N,bus,C}^{CHP}\right)}{\left(H_{N,bus,B}^{CHP} - H_{N,bus,C}^{CHP}\right)}\left(H_{N,bus,k}^{CHP} - H_{N,bus,B}^{CHP}\right) \geq \{-(1 - U_{bus,k}^{CHP})NL\} \quad (49)$$

$$P_{N,bus,k}^{CHP} - P_{N,bus,C}^{CHP} - \frac{\left(P_{N,bus,C}^{CHP} - P_{N,bus,D}^{CHP}\right)}{\left(H_{N,bus,C}^{CHP} - H_{N,bus,D}^{CHP}\right)}\left(H_{N,bus,k}^{CHP} - H_{N,bus,C}^{CHP}\right) \geq \{-(1 - U_{bus,k}^{CHP})NL\} \quad (50)$$

$$0 \leq H_{N,bus,k}^{CHP} \leq H_{N,bus,B}^{CHP} U_{bus,k}^{CHP} \quad (51)$$

$$0 \leq P_{N,bus,k}^{CHP} \leq P_{N,bus,A}^{CHP} U_{bus,k}^{CHP} \quad (52)$$

The area under the curve AB, BC and CD are modelled using Equations 19,20 and 21, respectively. The heat and power limits of CHP are set using Equations 22 and 23.

$$OF^{CHP}_{bus,k} = a^{CHP}(P^{CHP}_{N,bus,k})^2 + b^{CHP}P^{CHP}_{N,bus,k} + c^{CHP} +$$

$$\mathrm{d}^{CHP}(H^{CHP}_{N,bus,k})^2 + e^{CHP}H^{CHP}_{N,bus,k} + f^{CHP} \quad (53)$$

The controlling parameters of CHP data are given in Section 4.

8) ZIP Load Model

The voltage-dependent time-varying constant impedance (Z), constant current (I), and constant power (P) called ZIP [38] load is carried out for the analysis. The active power demand and reactive power demand is given in Equation 54-55.

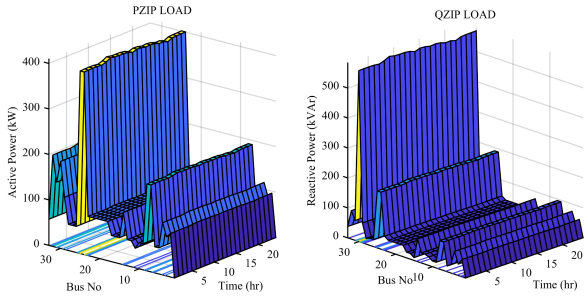

Figure 4. ZIP Load profile

$$P^{ZIP}_{i,k} = Pd_i\left[Z_p\left(\frac{V^k_i}{V^k_{min}}\right)^2 + I_p\left(\frac{V^k_i}{V^k_{min}}\right) + P_p\right] \quad (54)$$

$$Q^{ZIP}_{i,k} = Qd_i\left[Z_q\left(\frac{V^k_i}{V^k_{min}}\right)^2 + I_q\left(\frac{V^k_i}{V^k_{min}}\right) + P_q\right] \quad (55)$$

$\forall \ \{Z_i + I_i + P_i = 1\}$ Pd_i and $Qd_i$are the load demand at each bus i. The active and reactive part of ZIP load is shown in Figure 4.

9) Network Model

In this paper, the base Case model is considered the IEEE-33 standard bus test system. The different sources are connected, as shown in Figure 5. The FC at 25th bus, the WT at 30th bus, MT at 12th bus, CHP-1 at 5th and CHP-2 at 11th, PV and BES at 18th bus have been installed.

3. ALGORITHM

The algorithm consists of the two-layer model (outer and inner). The outer layer model consists of the iterative algorithm and the Mixed Integer non-linear programming (MINLP) approach to obtain the best size of BES. In

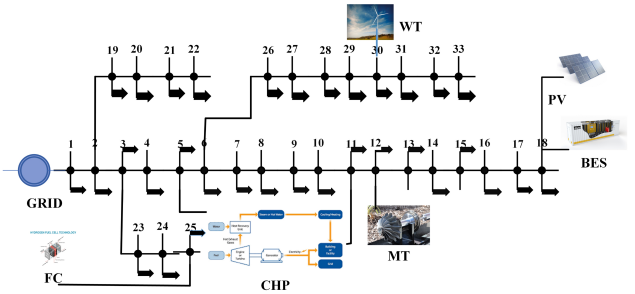

Figure 5. The network model for energy sources

the inner layer model, the optimization problem has been solved using (MINLP) approach for obtaining the battery charging/discharging power, state of charge (SOC) and other variables (Power output of generating units, voltage profile of network etc.) as explained in Section 2 The following algorithmic steps are used to solve the problem:

Step 1 Outer layer algorithm

1) Read the solar irradiation, wind speed data.
2) Run the MCS to obtain the PV and WT output.

Step 2 Distribution load flow

1) Read the IEEE-33 bus data.
2) Obtain the voltage profile for the base Case.
3) Calculate the voltage-dependent ZIP load parameters.

Step 3: Obtain the battery minimum ($Batt_{min}$) and maximum ($Batt_{max}$) size

1) Run the power flow for 24 hours ZIP load variation.
2) Obtain the bus location having the highest power losses. Mark the bus as a sensitive node to obtain daily energy loss.
3) Calculate the minimum and maximum battery size for the IEEE-33 bus network

Step 4: Solve the iteration for obtaining the optimal BES sizing and location as follows:

1) Set iteration =1 and $Batt_{size} = Batt_{min}$
2) Transfer all locations of buses from MATLAB to the GAMS environment.
3) Run the MINLP solver in GAMS to solve the objective Equations 1 and 2.
4) Calculate the battery cost per day Equation 4.
5) Execute the inner layer mode. Solve the UC and piece wise linear cost model from Equation 40 to 47.
6) Run the optimal power flow from Equation 7-10 to obtain the daily energy loss.
7) Run the iteration up to $Batt_{size} = Batt_{max}$
8) Transfer the obtained variables from GAMS to MAT-

LAB

9) Select the optimal size and location of BES for the inner layer model.

Step 5 Inner layer optimization:

1) Set the optimal battery size ($Batt_{size\_optimal}$) is $Batt_{size}$ from the outer layer model
2) Solve for Equation 6, for analysis of BES
3) Solve the UC and piecewise linear cost model from Equations 40 to 47 with considering the constraints from Equation 11 to 30 for the optimal scheduling and power output of generating units.
4) Obtain the charging/discharging power, state of charge (SOC) for BES
5) Run the optimal load flow from Equation 7-10 to obtain the voltage profile.

Step 6 Transfer the results obtained from GAMS to MATLAB.

Step 7 Print the results obtained in MATLAB.

Figure 6, depicts the flow chart of the proposed algorithm.

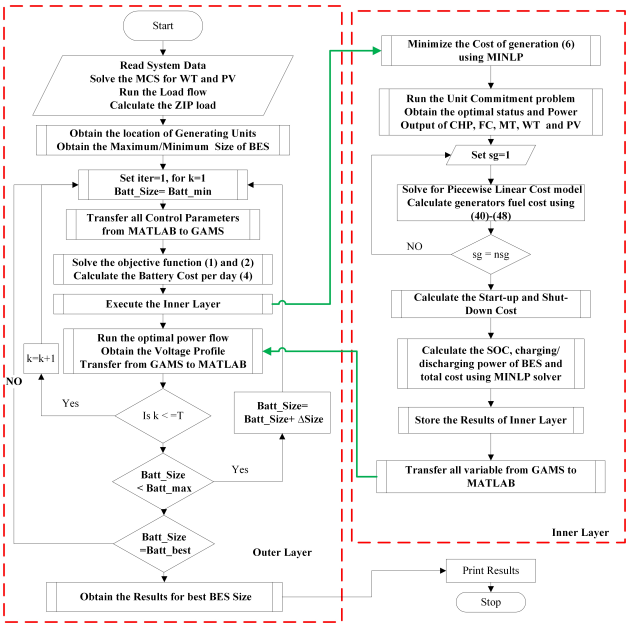

Figure 6. Proposed algorithm for the size of BES in MG

4. SYSTEM DATA

In this section, the system data is taken from [2]. The ZIP load data [8], coefficients of ZIP load, percentage of the demand and market price, FC and MT data, Solar PV and Wind data are taken from the literature [8]. The FC and MT power generation data [2] is taken from the literature [35]. The data for the CHP and market price for 24 hours are taken from the literature [8] for analysis.

A. Solar and Wind Turbine cost data

The BES, solar PV and wind cost-based data of Zaragoza (Spain) [18], [39] [40] [41] is given in Table I. The wind speed and solar irradiation data are taken from NASA meteorological data of Zaragoza (Spain).

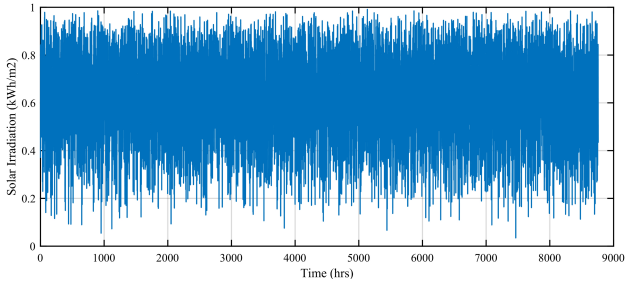

Figure 7. Hourly Solar irradiation of Zaragoza (Spain) [39] [40] [41]

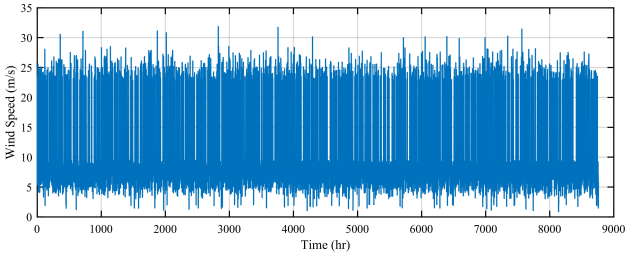

Figure 8. Hourly wind speed of Zaragoza (Spain) [39] [40] [41]

B. Data for the FC, MT and CHP

The MT and FC data is represented in Table II [2].

The data for CHP#1 and CHP#2 is given in Table III.

5. RESULTS AND DISCUSSIONS

The algorithmic steps are presented in Section 4 to solve the multi-objective problem. The three Cases are analyzed as follows:

Case 1: Size of battery energy storage (BES) considering CHP, FC, MT, WT and PV energy sources.

Case 2: The BES size considering CHP, FC, and MT.

Case 3: The MB has been determined without considering the battery energy storage.

A. Base Case

The IEEE-33 bus test system has been taken into account for the base Case. The peak load demand of the base Case is 3715+j2300 kVA, the minimum voltage is 0.91309 pu, and the power loss is 202.66+j135.13 kVA [43]. The peak load demand for the ZIP load for the 33-bus radial system is 3622.073+j2235.572 kVA [44] at the 7th hour, and the power loss is 199.3078+j135.0986 kVA. Whereas the daily energy loss is 4599.882+j3117.837 kVA, and the annual cost of energy loss is $ 100737.4 with the ZIP load for the base Case.

TABLE I. The cost data of PV, WT and BES [18], [39], [40], & [42]

Sources	Acquisition cost ($)	O&M ($/year/kW)	Replacement cost ($/Lifetime)	Lifespan (year)	Rating
PV	2400	18	2.95 @ 25 year (Life-time)	25	800 (kW)
WT	3724.5	31	3009.5	20	1000 (kW)
BES	600	20	4.64 @ 1.45 year	10	100 (kWh)

TABLE II. Parameters of MT and FC [2]

Type	a	b	c	Pmax	Pmin	RD	RU	DT	UT	CostST	CostSD	P10	R10	U0	SU
MT	0.001	0.52	60	1000	100	40	40	2	2	50.6	50.6	1000	500	2	140
FC	0.001	0.36	85	1000	100	30	30	0	0	57.1	57.1	1000	500	3	80

TABLE III. Data for the CHP unit 1 and unit 2

Type	a	b	c	CostST	Bp	d	e	f	RD	Bq
CHP#1	0.0345	14	254.0	47.9	215	0.03	4.2	0.031	40	180
CHP#2	0.0435	13	146.0	50.6	110	0.02	0.7	0.011	104	135
Type	Ap	Bp	Cp	Dp	CostSD	Aq	Bq	Cq	Dq	RU
CHP#1	247	215	81	99	47.6	0	180	104.8	0	40
CHP#2	125	110	40	45	50.6	0	135	75	0	104

B. Case 1

In this Case study, the CHP, FC, MT, WT and PV units are taken into account to obtain the BES size.

1) Result of the outer layer

Table IV gives the results for each battery size, battery cost, cost of UC, total benefit, and daily energy loss. These results have been obtained by solving the optimal load flow with the unit commitment problem (as explained in Section 2 in GAMS. The range of BES size is obtained between 900 kWh to 2800 kWh with 100 kWh increment. In Table IV, the maximum market benefit and total benefit obtained are $ 70666.19 and $ 69594.56, with a battery storage size of 1600 kWh, respectively. Therefore, the other cost variables obtained with the BES of 1600 kWh are: (i) the daily energy loss obtained is 1748.352 kWh (ii) battery cost per day obtained is $ 1071.631 and (iii) the generation cost for FC/MT/CHP, including with the total UC cost obtained is $ 193209.393.

On the other hand, in Table IV, the minimum energy loss per day obtained is 1690.896 kWh at a BES size of 2500 kWh. The total benefit and market benefit with BES size of 2500 kWh obtained are $ 64866.44 and $ 66540.86, respectively, which are lower considering the BES size of 1600 kWh. However, the minimum daily energy loss is obtained for the BES of 2500 kWh, but the maximum point of total benefit is obtained simultaneously for the BES size of 1600 kWh. Therefore, the BES size of 1600 kWh has been taken for the optimal size since it has the maximum market benefit and the maximum total benefit, respectively. Further analysis has been carried out with the battery storage size of 1600 kWh for Case-1.

2) Result of inner layer optimization

The results obtained in the outer layer have been transferred to the GAMS module, and the BESS size taken is 1600 kWh. The optimization is carried out in GAMS using CONOPT3 [44] solver.

a) Result of the UC

The optimal scheduling of dis-patchable units considering the BES size of 1600 kWh has given in Table V. In Table V, ‘0’ stands for OFF, and ‘1’ stands for ON status of the generating units.

The operating cost can be minimized using the shut down of some dispatchable units. Furthermore, the MT is remain shut down for the 1st and 2nd hours, the FC is being shut down for the 23rd and 24th hour. Whereas CHP1 and CHP2 are not being shut down for the entire duration to minimize the cost of generation from Equation 6, with the size BES size of 1600 kWh. In Figure 9, the startup cost (STC) of MT obtained is $ 50.6 at 3rd, 6th, 13th, and 21st hour since it started. Although the shutdown cost (SDC) of MT obtained is $ 50.6 at 4th, 8th and 17th hours, it is shut down. The FC unit remains ON, and it is being shut down at the 23rd hour. The SDC of FC obtained is $ 47.1 at the 23rd hour. The CHP units 12 are remained on for the entire duration; therefore, the STC and SDC of the CHP units are zero.

The unit spinning reserve capacity (Rn) has been shown in Figure 10 for the generating units.

The spinning reserve for the MT and FC with considering the PV, Wind and ZIP load. The total amount of

TABLE IV. Result for BES size

BES size (kWh)	Cost per day ($)	TB (Total benefit)($)	Market Benefit ($)	Daily Energy Loss (kWh)
900	602.7926	53200.56	53803.35	1983.072
1000	669.7696	40829.65	41499.41	1891.215
1100	736.7465	26178.22	26914.97	1932.271
1200	803.7235	67076.99	67880.71	1768.994
1300	870.7004	65085.41	65956.11	1765.236
1400	937.6774	-7336.71	-6399.04	2110.045
1500	1004.654	67031.34	68036	1765.305
1600	**1071.631**	**69594.56**	**70666.19**	**1748.352**
1700	1138.608	63577.74	64716.35	1802.383
1800	1205.585	59425.56	60631.15	1782.637
1900	1272.562	61739.53	63012.1	1767.012
2000	1339.539	64494.99	65834.53	1722.452
2100	1406.516	65931.78	67338.29	1709.862
2200	1473.493	69021.87	70495.36	1743.640
2300	1540.470	65322.81	66863.28	1707.500
2400	1607.447	66017.03	67624.47	1697.099
2500	**1674.424**	**64866.44**	**66540.86**	**1690.896**
2600	1741.401	-8727.36	-6985.96	2086.163
2700	1808.378	62353.58	64161.96	1728.626
2800	1875.355	64868.34	66743.70	1725.043

TABLE V. Schedule of dispatchable generators when the installation of 1600 kWh BES

Hour	MT	FC	CHP1	CHP2
1	0→0	1→1	1→1	1→1
2	0→0	1→1	1→1	1→1
3	0→1	1→1	1→1	1→1
4	1→0	1→1	1→1	1→1
5	0→0	1→1	1→1	1→1
6	0→1	1→1	1→1	1→1
7	1→1	1→1	1→1	1→1
8	1→0	1→1	1→1	1→1
9	0→0	1→1	1→1	1→1
10	0→0	1→1	1→1	1→1
11	0→0	1→1	1→1	1→1
12	0→0	1→1	1→1	1→1
13	0→1	1→1	1→1	1→1
14	1→1	1→1	1→1	1→1
15	1→1	1→1	1→1	1→1
16	1→1	1→1	1→1	1→1
17	1→0	1→1	1→1	1→1
18	0→0	1→1	1→1	1→1
19	0→0	1→1	1→1	1→1
20	0→1	1→1	1→1	1→1
21	1→1	1→1	1→1	1→1
22	1→1	1→1	1→1	1→1
23	1→1	1→0	1→1	1→1
24	1→1	0→0	1→1	1→1

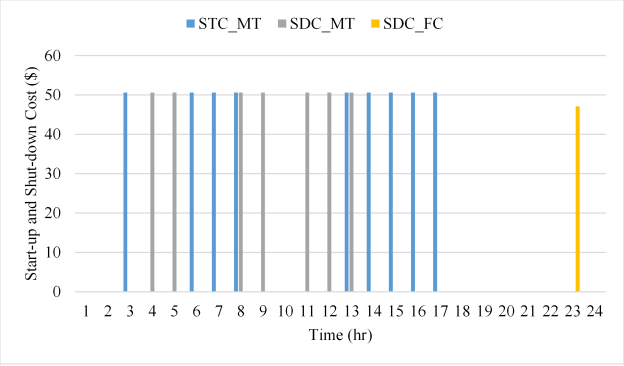

Figure 9. Startup and shut down the cost of the dispatchable unit for Case-1

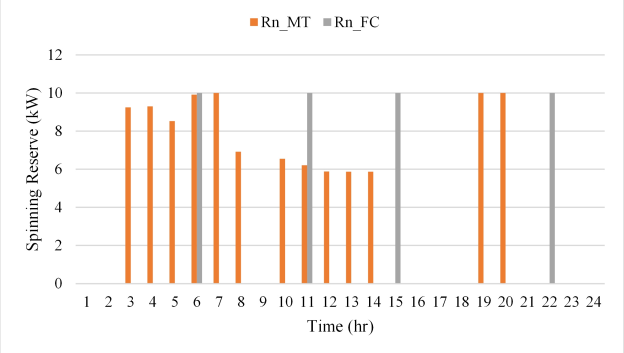

Figure 10. Spinning reserve for the dispatchable generator for Case-1

generation of FC and MT has been shown in Figure 10. 10, which includes the available energy stored in ESS minus the per-cent of ZIP load and losses being supplied. The spinning reserve of the CHP unit is not considered since the higher operational constraints and cost of generation.

b) Result for the BES for Case-1

In Figure 11, the SOC, charging and discharging power of BES is depicted.

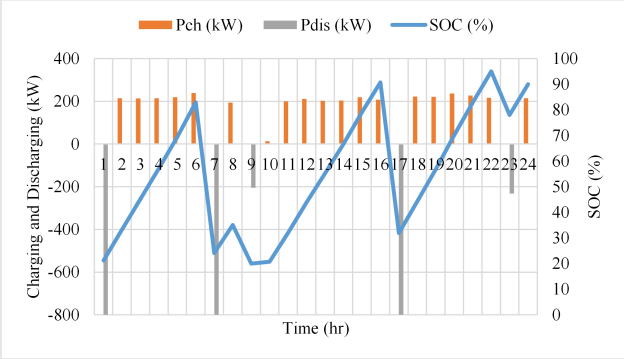

Figure 11. Charging/Discharging power, SOC of BES for Case-1

The percentage SOC is depicted in Figure 11 in the blue line, whereas green bars for charging power and red bars for battery storage discharging power. The power supplied by the BES is represented by negative power, whereas the power drawn by the BES is shown as positive power in Figure 11. The BES power (charging/discharging) depends on the availability of the generation. The Li-ion battery has been considered for analysis, the maximum depth of discharge of 0.8 is taken for the analysis [18]. The maximum charging and discharging power limit set is 50% of battery size. The initial set-point is 80% of BES size at 1st hour, whereas the final set-point is 90% at the 24th hour. The battery has supplied 800 kW at 1st hours since the lower power demand and maintains the SOC to 90% whereas it has to draw maximum power of 234.48 kW at 12th hours and 211.40585 kW at 13th hours from the point of common coupling (PCC) since the excess amount of supply.

c) The power output of generating units with BES for Case-1

Figure 12 shows the grid power and output power of RES. The optimal location and size of BES and PV are obtained at the 18th bus, whereas the two numbers of CHP units are installed at the 5th and 11th bus [1], MT at the 12th bus, WT at the 30th bus and FC at the 25th bus. In this context, the location of generating units are assumed and taken from the literature for the analysis.

In Table VI, the obtained size and location of energy sources are shown. The location of BES (1600 kWh) is

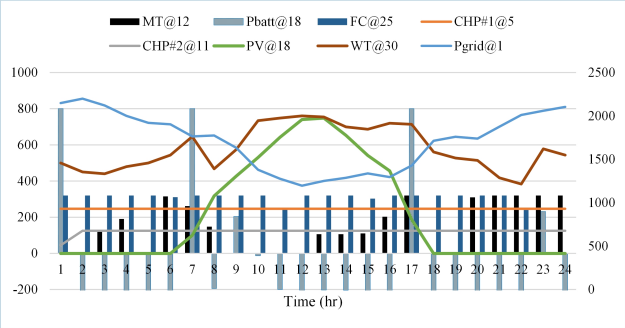

Figure 12. Power output profile for 24 hrs ZIP load variation

TABLE VI. Size and location of Energy Sources

Type	Location at bus	Max.Power Output (kW)
CHP#1	@ 5th bus number	247
CHP#2	@ 11th bus number	125
MT	@ 12th bus number	320
PV	@ 18th bus number	748
FC	@ 25th bus number	320
WT	@ 30th bus number	760

obtained at the 18th bus. The size of WT obtained is 760 kW for an hourly load variation. The maximum power output of 2199.484 kW is drawn from the upstream grid at the 2nd hour, since the lower price of electricity.

The maximum power output obtained is 760 kW for WT at the 12th hour for an hourly load variation.

d) Voltage Profile of Case-1

In Figure 13, Case-1 with the Base Case to obtain a voltage profile is depicted Figure 13. Voltage Profile for Case-1 with BES of 1600 kWh.

The Voltage profile has been enhanced for Case-1, concerning the Base Case. The minimum value of voltage (0.934807 pu) is obtained for the 2nd hour at the 18th bus.

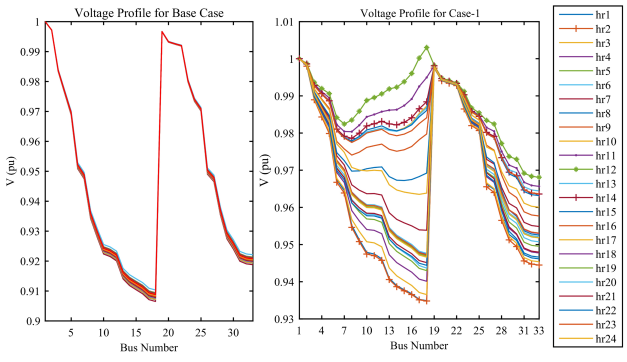

Figure 13. Voltage Profile for Case-1 with BES of 1600 kWh

The minimum voltage for the base Case obtained is

0.906493 pu. Therefore, the minimum voltage profile has been enhanced by 3.1234% with Case-1. The maximum value of voltage (1.003029 pu) is obtained at the 12th hour for the 18th bus since the installation of solar PV (748 kW) and BES (1600 kWh). The maximum voltage has been enhanced to 0.3029% with Case-1.

C. Case 2

In this Case study, the CHP+MT+FC units are considered to determine the sizing of BES. The impact of BES has been carried out with the dis-patchable units.

1) Results for the outer layer

In Table VII, the outer layer results are shown by considering the number of iterations for the BES sizing, battery cost per day, Total benefit, market benefit, and generation cost. The minimum value of BES size obtained is 1100 kWh, and the maximum value obtained is 2800 kWh.

In Table VII, the maximum increment of total benefit (TB) and the market benefit (MB) is the point of the maximum size of BES. The minimum decrement point of daily energy loss is also the point of the maximum size of BES. The maximum TB obtained of $ 60124.93 and the minimum daily energy loss of 2579.236 kWh are obtained at1200 kWh of BES size, respectively. Therefore, the obtained size of BES for Case-2 is 1200 kWh, at the point of maximum TB and the point of minimum daily energy loss. The annual cost of energy loss (CEL) has been reduced to $ 56485.27 with Case-2. Therefore the saving of CEL obtained is $ 44252.14.

2) Result of the inner layer model

In the previous section, BES of 1200 kWh size has the best results. Therefore, in this section, the impact of BES has been analyzed to obtain the optimal power output and scheduling of MT, CHP, and FC. The energy loss saving has also been determined.

a) Results for the UC

The BES size has been obtained by considering the UC problem for the optimal on/off status or scheduling of the dispatchable units. In this context, the minimum cost of UC for the dispatchable units along with the minimum daily energy loss have been carried out. Furthermore, the optimal on/off status of the MT, FC, and CHP units have been determined without considering the solar PV and WT.

Initially, the MT unit is OFF, and it is ON at 3rd hours to obtain the maximum benefit and minimum generation cost with the same constraints. The FC, CHP1, and CHP2 units remain ON for the entire duration since the solar PV and WT are not considered. Furthermore, the BES has been discharged for the first two hours to fulfil the demand since the MT unit is shut down for this duration. Moreover, the FC and CHP units are not kept OFF for the day-long since the PV and WT are not installed. The obtained STC of $ 50.6 for the MT at 3rd hour.

b) Result for the power output

In Figure 14, the MT is initially being OFF, and BES can deliver the necessary power with Case-1.

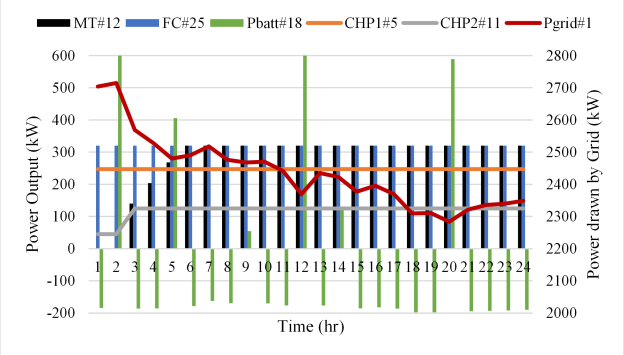

Figure 14. The power output of MT, FC, CHP1, and CHP2 with BES of 1200 kWh

The MT is ON at the 3rd hour, and it remains ON for the whole duration. Furthermore, the FC and CHP units 12 are not shut down since the PV and WT are not installed. The maximum power drawn by the grid is 2715.045 kW at 2nd hours to maximize the total benefit with the same constraints, since the lower value of the market price. In Figure 14, the maximum power output for CHP1 and CHP2 is 320 kW and 125 kW at the 5th and 11th bus, respectively, MT is 320 kW at the 12th bus, FC is 320 kW at 25th bus.

c) Results for the Battery storage

The Li-ion battery energy storage has been used for the analysis since the lower depth of discharge rate is about 0.3 and better degradation factor and lower maintenance cost. In this contrast, the maximum discharging/charging power is taken at 50% of the battery full capacity. In Figure 15, the battery charging/discharging power, along with the state charge of battery storage, is shown.

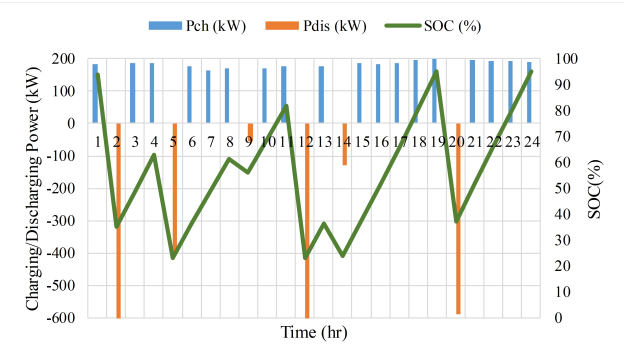

Figure 15. The battery power profile of size 1200 kWh

The minimum and maximum set-points of SOC are

TABLE VII. Results for outer layer of Case-2

BES size (kWh)	Cost per day ($)	TB (Total benefit)($)	Market Benefit ($)	Daily Energy Loss (kWh)
1100	736.7465	52499.59	53236.33	2675.254
1200	**803.7235**	**60124.93**	**60928.65**	**2579.236**
1300	870.7004	59998.34	60869.04	2579.388
1400	937.6774	59960.06	60897.73	2580.015
1500	1004.654	59855.62	60860.27	2580.96
1600	1071.631	59788.64	60860.27	2582.154
1700	1138.608	59699.02	60837.63	2583.440
1800	1205.585	59636.59	60842.18	2584.728
1900	1272.562	59591.38	60863.95	2586.019
2000	1339.539	59504.07	60843.61	2587.313
2100	1406.516	59449.31	60855.83	2588.608
2200	1473.493	59378.15	60851.64	2589.907
2300	1540.47	59297.65	60838.12	2591.207
2400	1607.447	59227.30	60834.74	2592.510
2500	1674.424	59157.13	60831.55	2593.815
2600	1741.401	59092.76	60834.16	2595.123
2700	1808.378	58958.9	60767.28	2596.433
2800	1875.355	24048.6	25923.96	2843.282

taken as 20% and 95% respectively, for the safe mode of operation of BES. Initially, the battery SOC is set at 80% of the total capacity. The battery gets discharged at the 2nd hour since the load demand is higher and again charged at the 3rd hour since the availability of excess power.

d) Voltage profile of Case-2

The voltage profile for Case-2 for the hourly ZIP load is shown in Figure 16.

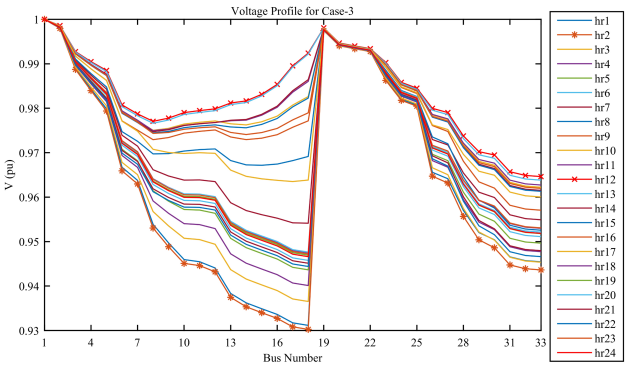

Figure 16. Voltage profile for Case-2 with BES size of 1200 kWh

The minimum value of the voltage (0.923284 pu) for Case 2 is obtained at the 2nd hour for the 18th bus. The maximum voltage profile has been obtained at 20th hours since the BES delivered 588.8004 kW at this duration with Case-2.

D. Results of Case 3

In this Case study, the BES has not been considered for the analysis. Therefore, the outer and inner layers models do not contain the number of iterations as in the previous Case study of Case-1 and Case-2. The renewable-based energy sources (PV/WT/MT/FC/ CHP) have been taken into account without BES. The total benefit obtained is $ 62449.43 for Case-3 without BES, whereas the market benefit obtained is $ 69594.56 for Case-1 with BES. Therefore, TB is increased to $ 7145.133 for Case-1 with BES.

1) Results for the UC

The multi-objective problem has been solved by considering the optimal scheduling of sources without BES.

The MT starts at the 3rd hour, since the lower load demand. The startup cost of generation obtained is $ 50.6 for the MT at 3rd hour. The MT is supplying the power for the remaining hours. The FC and CHP of units 1& 2 are ON for the whole day long to maintain the power supply for the demand. The optimal scheduling for the generating units is given in Table VIII.

In Figure 17, the MT is being started up at the 3rd hour, at the 11th hour, the MT is being shut down, and it again starts at the 14th hour to maintain the same constraints. Moreover, the MT is being shut down from the 12th hour to the 14th hour since the required demand has been supplied with solar PV for the duration.

2) Results of the power output for Case-3

The power output profile of PV, WT, FC, MT and CHP units are shown in Figure 18, without BES. The maximum power output for solar PV of 750 kW at 18th bus, WT of 760 kW at 30th bus, MT of 320 kW at 12th bus, FC 0f 320 kW at 25th bus, CHP#1 of 247 kW at 5th bus, and CHP#2 of 125 kW at 11th bus has been obtained without BES.

The maximum power drawn from the grid is 2233.784

TABLE VIII. Status of dispatchable units when 1200 kWh BES installed

Hour	MT	FC	CHP1	CHP2
1	0→0	1→1	1→1	1→1
2	0→0	1→1	1→1	1→1
3	0→1	1→1	1→1	1→1
4	1→1	1→1	1→1	1→1
5	1→1	1→1	1→1	1→1
6	1→1	1→1	1→1	1→1
7	1→1	1→1	1→1	1→1
8	1→1	1→1	1→1	1→1
9	1→1	1→1	1→1	1→1
10	1→1	1→1	1→1	1→1
11	1→0	1→1	1→1	1→1
12	0→0	1→1	1→1	1→1
13	0→0	1→1	1→1	1→1
14	0→1	1→1	1→1	1→1
15	1→1	1→1	1→1	1→1
16	1→1	1→1	1→1	1→1
17	1→1	1→1	1→1	1→1
18	1→1	1→1	1→1	1→1
19	1→1	1→1	1→1	1→1
20	1→1	1→1	1→1	1→1
21	1→1	1→1	1→1	1→1
22	1→1	1→1	1→1	1→1
23	1→1	1→1	1→1	1→1
24	1→1	1→1	1→1	1→1

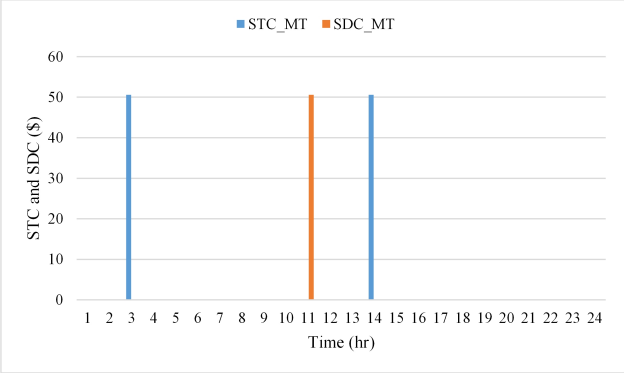

Figure 17. Startup and shut down the cost of MT unit

kW at 2nd hour of the lower price of electricity. The minimum power drawn from the grid is 1154.941 kW at the 12th hour since the intermittent nature of solar PV fulfils the load demand. Therefore, the power drawn from the grid is lower when the solar PV and WT has supplied the power vice versa.

3) Results of Voltage profile for Case-3

In Figure 19, the voltage variation is depicted for 24-hour ZIP load. The minimum value of 0.93025 pu voltage is obtained at the 2nd hour for the 18th bus, which is increased to 2.3757% concerning the base Case.

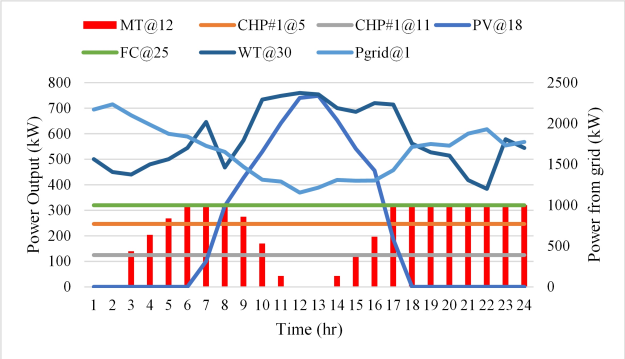

Figure 18. Power Output of Renewable Generation without energy storage

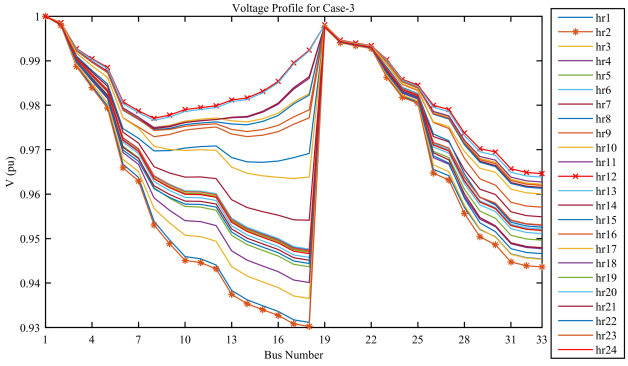

Figure 19. Voltage Profile for 33 bus system with 24 hours ZIP load variation without BES

E. Voltage and Power loss Profile

The minimum voltage and power loss profile for the Base Case, Case-1 and Case-2, is shown in Figure 20. In Figure 20, the voltage profile for a minimum value of the 33-bus test system is shown. The voltage profile has been improved for Case-1. However, in Case-3, the voltage is slightly reduced with Case-1 since the BES has been installed at the 18th bus for Case-1. The voltage profile for Case-2 is not so impressive since the PV and WT have not been installed. The minimum voltage is obtained at the 18th

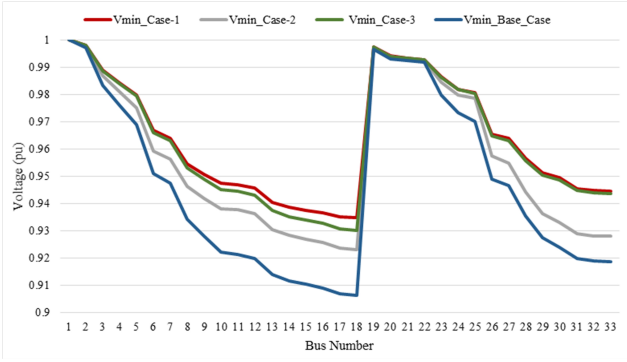

Figure 20. Minimum voltage profile for the Base Case, Case-1, Case-2 and Case-3 for the 33-bus system

bus for each Case study. Furthermore, the minimum voltage value obtained is 0.934807046 pu (Case-1), 0.923283898 pu (Case-2), 0.93024998 pu (Case-3), and 0.906493272 pu (Base Case). Therefore the minimum value of voltage enhanced for Case-1 is 0.455% with Case-3 using the BES. Therefore, in Case-1 with BES, the minimum voltage has been improved by 0.455% with Case-3 (without using BES). Moreover, the minimum voltage has been improved for Case-1 by 2.83 % with the base Case.

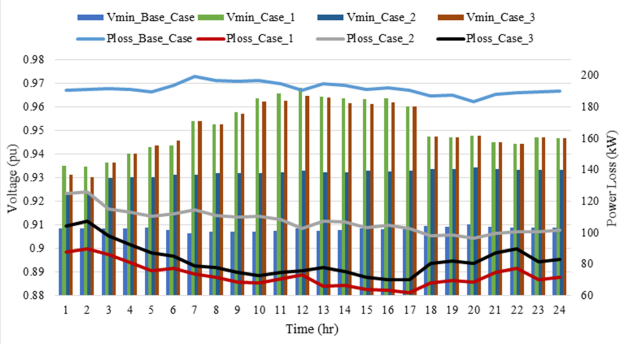

Figure 21. Hourly Minimum voltage and power loss profile for all Cases without BES

The hourly power loss profile is shown in Figure 21. The higher value of minimum voltage obtained is 0.968104 pu for the Case-1 at 12th hour, 0.934371 pu for Case-2 at the 20th hour and 0.909368 pu for the base Case at the 20th hour. Therefore, the minimum voltage has been enhanced for Case-1 by 5.77% and for Case-2 by 2.404% concerning the base Case since the PV and WT have been installed in Case-1.

The voltage profile has been enhanced with Case-1 and Case-3 since the solar PV was simultaneously installed at the 18th bus. Furthermore, the total power loss profile for 24 hours load variation is shown in Figure 21. The power loss is enhanced for Case-1 and Case-3 since installing PV at the 18th bus and WT at the 30th bus test system. Therefore the minimum power loss has been obtained for Case-1. The daily energy loss obtained is 1748.352 kWh for Case-1, 2579.236 kWh for Case-2, and 1980.640 kWh for Case-3. Therefore the daily energy loss is improved for Case-1 to 61.99% with the base Case.

6. CONCLUSION

The optimal size of BESS has been obtained with renewable energy sources. The modified IEEE -33 bus considering the time-varying realistic load model, has been successfully tested with the proposed system. Based on the obtained results, the following points are concluded as follows;

- It is concluded that the maximum amount for Market benefit, Total benefit and the annual cost of energy loss saving have been obtained with Case-1 overall Case studies. The results are compared with BES and without BES (Case-3) as follows; (i) the increment of TB with BES of 1600 kWh obtained is 11.44% (ii) The annual saving of CEL is increased by 11.72%Furthermore, the increment in voltage profile obtained is 0.455%Therefore, the impact of BES has better results over the distribution network in terms of the total benefit, annual CEL saving, and the improvement of voltage profile also.
- It is concluded that the best results have been obtained with Case1 over Case 2 in terms of TB, MB, annual CEL, and voltage profile enhancement. In addition, the results for Case-1 has advantages over Case-2 as follows; (i) The TB and MB are increased to 9469.63*and*9737.54, respectively. (ii) The annual cost of energy-saving is increased by 32.21%(iii) The minimum voltage has been enhanced by 1.152% with Case-1.

The BES size of 1600 kWh and 1200 kWh are obtained for Case-1, and Case-2, respectively. Furthermore, the simulation has been solved in the 64-bit operating system, Windows 10, with an i7 Processor Speed of 3.4 GHz. The proposed algorithm has taken the simulation time is 13.932627 seconds.

REFERENCES

[1] H. T. Le and T. Q. Nguyen, "Sizing energy storage systems for wind power firming: An analytical approach and a cost-benefit analysis," in *2008 IEEE Power and Energy Society General Meeting-Conversion and Delivery of Electrical Energy in the 21st Century*. IEEE, 2008, pp. 1–8.

[2] S. X. Chen, H. B. Gooi, and M. Wang, "Sizing of energy storage for microgrids," *IEEE transactions on smart grid*, vol. 3, no. 1, pp. 142–151, 2011.

[3] B. Bahmani-Firouzi and R. Azizipanah-Abarghooee, "Optimal sizing of battery energy storage for micro-grid operation management using a new improved bat algorithm," *International Journal of Electrical Power & Energy Systems*, vol. 56, pp. 42–54, 2014.

[4] W. Su, J. Wang, and J. Roh, "Stochastic energy scheduling in microgrids with intermittent renewable energy resources," *IEEE Transactions on Smart grid*, vol. 5, no. 4, pp. 1876–1883, 2013.

[5] V. M. Vallem and A. Kumar, "Retracted: Optimal energy dispatch in microgrids with renewable energy sources and demand response," *International transactions on electrical energy systems*, vol. 30, no. 5, p. e12328, 2020.

[6] Y. Zhang, Y. Xu, H. Yang, and Z. Y. Dong, "Voltage regulation-oriented co-planning of distributed generation and battery storage in active distribution networks," *International Journal of Electrical Power & Energy Systems*, vol. 105, pp. 79–88, 2019.

[7] M. Jadidbonab, B. Mohammadi-Ivatloo, M. Marzband, and P. Siano, "Short-term self-scheduling of virtual energy hub plant within thermal energy market," *IEEE Transactions on industrial electronics*, vol. 68, no. 4, pp. 3124–3136, 2020.

[8] F. Nazari-Heris, B. Mohammadi-ivatloo, and D. Nazarpour, "Network constrained economic dispatch of renewable energy and chp

TABLE IX. List of Symbols

P_{solar}	Solar output power
UCC_{disp}	Unit Commitment Cost
$Rn_{i,k}$	Spinning reserve
V	Rated Voltage
$U_{i,k}^{PV}, U_{i,k}^{wind}$	On/Off status of PV and WT
k	Time index
$P_{dis_i}^{k}$	Power discharge (BES)
$P_{ch_i}^{k}$	Power charge (BES)
S_T	Set of time k
i	Index for bus
S_B	Set of Battery location
nb	Total number of buses
$U_{bus,k}^{CHP}$	On/Off status of CHP unit
UCC_{disp}	Unit Commitment Cost
$Rn_{i,k}$	Spinning reserve
$P_{i,k}^{wind}$	Power output of Wind Turbine
$voll^{wind}, voll^{PV}$	Value of loss for WT and PV
$P_{gen_i}^{k}$	Active Power output for generating unit
$Q_{gen_i}^{k}$	Reactive Power output for generating unit
$P_{gen_{i,k}}^{max}$	Maximum power limits
$P_{gen_{i,k}}^{min}$	Minimum power limits
NL	Largest unit
$Pgrid_i^k$	Power is drawn from the grid
$Batt_{CPD}$	Per day cost of battery
rt	Interest rate
yr	Years
$Batt_{fc}$, $Batt_{MC}$	Fixed and maintenance cost of battery
SOC_{min}	State of Charge (minimum)
SOC_{max}	State of Charge (Maximum)
N_{batt}	Number of BES
δd	Depth Of Discharge
P_{ch}	Power (charging)
P_{dis}	Power (discharging)
η_{ch}	Efficiency (charging)
η_{dis}	Efficiency (discharging)
$E_{ch_{i,k}}^{min}$	Min. BES charging energy
$E_{dis_{i,k}}^{min}$	Min. BES discharging energy
$G0$	Standard Solar irradiation ($\frac{watt}{m^2}$)
P_{rated}^{PV}	PV rated power
N_{PV}	Total number of PV panel
$P_{i,k}^{wind}$	Wind output power
N_{wind}	Number of wind Turbine
v_{in}	Velocity of wind (Cut-in) in m/s
v_{out}	Velocity of wind (Cut-out) in m/s
nsg	number of segments
$Cost_{gen_{i,k,ini}}^{sg}$	Initial cost of segments
$Cost_{gen_{i,k,final}}^{sg}$	Final cost of segments
$Cost_{fuel}^{gen}$	Fuel cost of generating units
a_i, $b_i$and c_i	Cost coefficient of generating units
A, B, C, D	Operating Points of the CHP
a^{CHP}, b^{CHP}, c^{CHP}, d^{CHP}, e^{CHP} and f^{CHP}	Cost coefficient for CHP
Pl_{max}^{k}	Maximum apparent power

based microgrids," *International Journal of Electrical Power & Energy Systems*, vol. 110, pp. 144–160, 2019.

[9] H. Hosseinnia, V. Talavat, and D. Nazarpour, "Effect of considering demand response program (drp) in optimal configuration of combined heat and power (chp)," *International Journal of Ambient Energy*, vol. 42, no. 6, pp. 612–617, 2021.

[10] J. Wang, H. Zhong, Q. Xia, C. Kang, and E. Du, "Optimal joint-dispatch of energy and reserve for cchp-based microgrids," *IET Generation, Transmission & Distribution*, vol. 11, no. 3, pp. 785–794, 2017.

[11] M. Alipour, B. Mohammadi-Ivatloo, and K. Zare, "Stochastic scheduling of renewable and chp-based microgrids," *IEEE Transactions on Industrial Informatics*, vol. 11, no. 5, pp. 1049–1058, 2015.

[12] Ö. P. Akkaş and E. Çam, "Optimal operational scheduling of a virtual power plant participating in day-ahead market with consideration of emission and battery degradation cost," *International Transactions on Electrical Energy Systems*, vol. 30, no. 7, p. e12418, 2020.

[13] G. Coppez, S. Chowdhury, and S. Chowdhury, "Battery storage and testing protocols for chp systems," in *2011 IEEE Power and Energy Society General Meeting*. IEEE, 2011, pp. 1–7.

[14] K. Zhou, J. Pan, and L. Cai, "Indirect load shaping for chp systems through real-time price signals," *IEEE Transactions on Smart Grid*, vol. 7, no. 1, pp. 282–290, 2015.

[15] X. Wang, M. Yue, E. Muljadi, and W. Gao, "Probabilistic approach for power capacity specification of wind energy storage systems," *IEEE transactions on industry applications*, vol. 50, no. 2, pp. 1215–1224, 2013.

[16] D. Fioriti and D. Poli, "A novel stochastic method to dispatch microgrids using monte carlo scenarios," *Electric Power Systems Research*, vol. 175, p. 105896, 2019.

[17] Y. Atwa, E. F. El-Saadany, M. Salama, R. Seethapathy, M. Assam, and S. Conti, "Adequacy evaluation of distribution system including wind/solar dg during different modes of operation," *IEEE Transactions on Power systems*, vol. 26, no. 4, pp. 1945–1952, 2011.

[18] M. H. Mostafa, S. H. A. Aleem, S. G. Ali, A. Y. Abdelaziz, P. F. Ribeiro, and Z. M. Ali, "Robust energy management and economic analysis of microgrids considering different battery characteristics," *IEEE Access*, vol. 8, pp. 54 751–54 775, 2020.

[19] S. Rajamand, "Cost reduction in microgrid using demand response program of loads and uncertainty modeling with point estimation method," *International transactions on electrical energy systems*, vol. 30, no. 4, p. e12299, 2020.

[20] V. Kumar and A. Murty, "Multi-objective energy management in microgrids with hybrid energy sources and battery energy storage systems," *Prot Control Mod Power Syst*, 2020.

[21] L. Ma, N. Liu, J. Zhang, W. Tushar, and C. Yuen, "Energy management for joint operation of chp and pv prosumers inside a grid-connected microgrid: A game theoretic approach," *IEEE Transactions on Industrial Informatics*, vol. 12, no. 5, pp. 1930–1942, 2016.

[22] J. Tang, M. Ding, S. Lu, S. Li, J. Huang, and W. Gu, "Operational flexibility constrained intraday rolling dispatch strategy for chp microgrid," *IEEE Access*, vol. 7, pp. 96 639–96 649, 2019.

[23] G. Zhang, Z. Shen, and L. Wang, "Online energy management for microgrids with chp co-generation and energy storage," *IEEE transactions on control systems technology*, vol. 28, no. 2, pp. 533–541, 2018.

[24] M. Emmanuel, R. Rayudu, and I. Welch, "Grid capacity released analysis and incremental addition computation for distribution system planning," *Electric Power Systems Research*, vol. 152, pp. 105–121, 2017.

[25] M. Resener, S. Haffner, L. A. Pereira, and P. M. Pardalos, "Mixed-integer lp model for volt/var control and energy losses minimization in distribution systems," *Electric Power Systems Research*, vol. 140, pp. 895–905, 2016.

[26] O. M. Mikic, "Variance-based energy loss computation in low voltage distribution networks," *IEEE Transactions on Power Systems*, vol. 22, no. 1, pp. 179–187, 2007.

[27] S. Sultana and P. K. Roy, "Multi-objective quasi-oppositional teaching learning based optimization for optimal location of distributed generator in radial distribution systems," *International Journal of Electrical Power & Energy Systems*, vol. 63, pp. 534–545, 2014.

[28] A. G. Tsikalakis and N. D. Hatziargyriou, "Centralized control for optimizing microgrids operation," in *2011 IEEE power and energy society general meeting*. IEEE, 2011, pp. 1–8.

[29] C. Abbey and G. Joós, "A stochastic optimization approach to rating of energy storage systems in wind-diesel isolated grids," *IEEE Transactions on power systems*, vol. 24, no. 1, pp. 418–426, 2008.

[30] V. Mohan, J. G. Singh, and W. Ongsakul, "An efficient two stage stochastic optimal energy and reserve management in a microgrid," *Applied energy*, vol. 160, pp. 28–38, 2015.

[31] P. Fortenbacher, J. L. Mathieu, and G. Andersson, "Modeling and optimal operation of distributed battery storage in low voltage grids," *IEEE Transactions on Power Systems*, vol. 32, no. 6, pp. 4340–4350, 2017.

[32] R. Levy, A. Brodsky, and J. Luo, "Decision guidance framework to support operations and analysis of a hybrid renewable energy system," *Journal of Management Analytics*, vol. 3, no. 4, pp. 285–304, 2016.

[33] E. Kuznetsova, Y.-F. Li, C. Ruiz, and E. Zio, "An integrated framework of agent-based modelling and robust optimization for microgrid energy management," *Applied Energy*, vol. 129, pp. 70–88, 2014.

[34] C. L. Borges and D. M. Falcao, "Optimal distributed generation allocation for reliability, losses, and voltage improvement," *International Journal of Electrical Power & Energy Systems*, vol. 28, no. 6, pp. 413–420, 2006.

[35] B. Singh and A. K. Sharma, "Optimal placement of dg with battery energy storage using cpls and combined dispatch strategy," in *Advances in Renewable Energy and Sustainable Environment*. Springer, 2021, pp. 317–325.

[36] A. C. Rueda-Medina, J. F. Franco, M. J. Rider, A. Padilha-Feltrin, and R. Romero, "A mixed-integer linear programming approach for optimal type, size and allocation of distributed generation in radial

distribution systems," *Electric power systems research*, vol. 97, pp. 133–143, 2013.

[37] A. Soroudi, *Power system optimization modeling in GAMS*. Springer, 2017, vol. 78.

[38] P. Kundur, "Power system stability," *Power system stability and control*, pp. 7–1, 2007.

[39] L. A. Bird, K. S. Cory, and B. G. Swezey, "Renewable energy price-stability benefits in utility green power programs," National Renewable Energy Lab.(NREL), Golden, CO (United States), Tech. Rep., 2008.

[40] I. Irena, "Renewable power generation costs in 2017. report," 2018.

[41] R. K. Jain, J. Qin, and R. Rajagopal, "Data-driven planning of distributed energy resources amidst socio-technical complexities," *Nature Energy*, vol. 2, no. 8, pp. 1–11, 2017.

[42] Y. Zhang, Y. Xu, H. Yang, and Z. Y. Dong, "Voltage regulation-oriented co-planning of distributed generation and battery storage in active distribution networks," *International Journal of Electrical Power & Energy Systems*, vol. 105, pp. 79–88, 2019.

[43] V. V. S. N. Murty and A. Kumar, "Impact of d-statcom in distribution systems with load growth on stability margin enhancement and energy savings using pso and gams," *International Transactions on Electrical Energy Systems*, vol. 28, no. 11, p. e2624, 2018.

[44] N. C. Koutsoukis, P. S. Georgilakis, and N. D. Hatziargyriou, "Multistage coordinated planning of active distribution networks," *IEEE Transactions on Power Systems*, vol. 33, no. 1, pp. 32–44, 2017.

Bharat Singh Bharat Singh is pursuing his Ph.D. from NIT Kurukshetra. He completed his B.Tech from GBPIET, UK, in 2012 and completed his PG from NIT HAMIRPUR, in Power System. He is currently working on the BES at the MG level. He has more than 6 Research papers in this field.

Dr. Ashwani K. Sharma Dr. Ashwani Kumar Sharma is presently a Professor Head in the Department of Electrical Engineering at NIT- Kurukshetra, Haryana. He received his B.Tech from Pant Nagar University in 1988 in Electrical Engineering and Master degree in Power Systems from Panjab University, Chandigarh in 1994 in honours and Ph.D. from IIT Kanpur in 2003. He did Post-Doctoral from Tennessee Technological University, USA. His research interest includes Power Systems, restructuring issues, Demand-side management, Smart grid technologies and Ancillary services.